RANSAC-Based Signal Denoising Using Compressive Sensing

Ljubiša Stanković[1] · **Miloš Brajović**[1] · **Isidora Stanković**[1] · **Jonatan Lerga**[2] · **Miloš Daković**[1]

Abstract

In this paper, we present an approach to the reconstruction of signals exhibiting sparsity in a transformation domain, having some heavily disturbed samples. This sparsity-driven signal recovery exploits a carefully suited random sampling consensus (RANSAC) methodology for the selection of a subset of inlier samples. To this aim, two fundamental properties are used: A signal sample represents a linear combination of the sparse coefficients, whereas the disturbance degrades the original signal sparsity. The properly selected samples are further used as measurements in the sparse signal reconstruction, performed using algorithms from the compressive sensing framework. Besides the fact that the disturbance degrades signal sparsity in the transformation domain, no other disturbance-related assumptions are made—there are no special requirements regarding its statistical behavior or the range of its values. As a case study, the discrete Fourier transform is considered as a domain of signal sparsity, owing to its significance in signal processing theory and applications. Numerical results strongly support the presented theory. In addition, the exact relation for the signal-to-noise ratio of the reconstructed signal is also presented. This simple result, which conveniently characterizes the RANSAC-based reconstruction performance, is numerically confirmed by a set of statistical examples.

Keywords Sparse signals · Robust signal processing · RANSAC · Impulsive noise · Compressive sensing · Sample selection · DFT

1 Introduction

In recent years, the reconstruction of sparse signals, based on a reduced set of random measurements, attracted significant research interest [3–7,10,12–15,17,19,20,22, 26,29,33,34,36–38,40–50,52,53,55,58]. Within the compressive sensing (CS) framework, a rigorous mathematical foundation has been established to support this type

---

🦎 Birkhäuser

of reconstruction, including the conditions that guarantee a successful and unique reconstruction result [6,49]. The most important requirement imposed by this theory is that the signal must be sparse in a particular transformation domain. Such signals are characterized by a small number of nonzero elements in the sparsity domain as compared to the full signal length and do appear in various applications [49]. Linear combinations of such coefficients represent compressive sensing measurements. Within the compressive sensing theory, highly effective algorithms for the sparse signal recovery have been supported by a well-defined mathematical framework [6,49]. These algorithms aim at minimizing sparsity measures under conditions posed by the measurements equations. The CS theory consistently characterizes the phenomena related with the reduced set of measurements [49]. The missing observations can be a result of physical unavailability, restrictions in the sensing process or restrictions posed by some physical phenomena. Highly corrupted signal samples, such as those being affected by the impulsive noise, can be also treated as unavailable and recovered using the CS techniques [49].

Signal samples in the time domain, being linear combinations of the sparsity domain coefficients, can be considered as the measurements within the CS framework. The number of samples required for the reconstruction is closely related to the number of nonzero coefficients in the sparse domain [6,13,49]. It has been repeatedly confirmed that in the case of heavily disturbed samples (outliers), it is preferable to omit these samples in both signal analysis and processing [50,51]. In the CS and sparse signal processing context, this means that the uncorrupted or low-corrupted samples (inliers) are considered as available measurements, whereas the heavily corrupted samples are considered as unavailable, and are reconstructed by applying some of the CS-based recovery algorithms. This further implies that a detection method shall be applied to identify the highly corrupted samples prior to their reconstruction [49]. One such methodology, founded on the signal sparsity principles, is presented in this paper. In contrast to the methods that combine the robust estimation and the CS-based signal recovery, the proposed method can provide an exact reconstruction if the reduced set of inliers is noise free, rather than to obtain a filtered approximation of the original signal [1,9,12,30,31,54,57].

The proposed algorithm is based on a random selection of subsets of signal samples (random sampling consensus—RANSAC) and a detection of the event when a disturbance-free (or low-corrupted) subset is selected. The RANSAC-based approach improves our detection and reconstruction based on sparsity measures, reported in [45], in the way that it provides a criterion to properly choose the best and largest possible set of adequate measurements—inliers, which are suitable for the CS-based reconstruction of corrupted samples—outliers [18]. The RANSAC approach is widely known for its outlier removal capabilities, commonly exploited in machine learning and computer vision [25,28,56], image registration [16,23] and other frameworks requiring robust estimation in the presence of outliers [11]. The signal-to-noise ratio (SNR) analysis in the CS-based reconstruction [44,47,49] shows that the quality of the reconstruction is directly influenced by the number of available samples. The presented RANSAC-based methodology is additionally equipped with the analysis of noise influence to the reconstructed signal, using an exact and simple relation for the SNR in the resulting signal.

The most important difference between the presented method and other methods that combine the robust estimation and the CS recovery is the assumption that we cannot distinguish the corrupted samples from the uncorrupted ones, based on their values [1,9,12,30,31,54,57]. During the last decades, blind denoising has been studied, among other areas, in the context of audio signal processing [2,5,8,27,32,35,41]. In our previous works with the audio signal denoising [5,41], we made extensive comparisons of CS-based denoising [41] and alternative sparsity-driven blind denoising [5] techniques for audio signals with the denoising approaches based on classical and sophisticated techniques founded upon the auto-regressive or other more advanced signal models [8,27]. The presented RANSAC-based approach delivers improved blind denoising performance in the context of audio signal processing, as techniques from [5,41], while bringing significant improvements in numerical efficiency of the process.

The paper is organized as follows: After the introduction, the background of the compressive sensing theory and the RANSAC overview are presented in Sect. 2. The denoising procedure based on the RANSAC is presented in Sect. 3, which also includes the discussion regarding the numerical complexity. The presented theory is verified numerically in Sect. 4, while the paper ends with some concluding remarks.

2 Definitions

Consider a signal $x(n)$ with N samples in the discrete-time domain. Assume that the sparsity domain of the signal is the discrete Fourier transform (DFT) domain. The signal and the DFT coefficients are related via

$$X(k) = \text{DFT}\{x(n)\} = \sum_{n=0}^{N-1} x(n)\varphi_k^*(n), \tag{1}$$

$$x(n) = \text{IDFT}\{X(k)\} = \frac{1}{N} \sum_{k=0}^{N-1} X(k)\varphi_k(n) \tag{2}$$

or $\mathbf{X} = \mathbf{W}\mathbf{x}$ and $\mathbf{x} = \mathbf{W}^{-1}\mathbf{X}$, where the basis functions take the form $\varphi_k(n) = \exp(j2\pi nk/N)$. In the matrix notation, the N-dimensional vector $\mathbf{X}$ has elements $X(k)$, vector $\mathbf{x}$ has elements $x(n)$, and the $N \times N$ transformation matrix $\mathbf{W}$ is with elements $\varphi_k^*(n)$, $k = 0, 1, \ldots, N-1$, $n = 0, 1, \ldots, N-1$.

The time-domain representation of a signal which is sparse in the DFT domain reads

$$x(n) = \sum_{i=1}^{K} A_i \varphi_{k_i}(n), \tag{3}$$

where A_i, $i = 1, 2 \ldots, K$, represent the nonzero elements at the transformation domain positions k_i, $i = 1, 2, \ldots, K$. The sparsity of this signal is K, $(K \ll N)$.

Assume that there are M available samples at the instants n_i, $i = 1, 2, \ldots, M$. In the CS theory, the linear combinations of the sparsity coefficients are referred to as the

measurements. Therefore, the available signal samples can be considered as the CS measurements, $y(i) = x(n_i)$. The measurement vector is denoted by **y**. Its elements are

$$y(i) = x(n_i) = \frac{1}{N} \sum_{k=0}^{N-1} X(k)\varphi_k(n_i), \quad i = 1, 2, \ldots, M. \tag{4}$$

The corresponding system of M equations with N unknowns is

$$a_{1,0}X(0) + a_{1,1}X(1) + \cdots + a_{1,N-1}X(N-1) = y(1)$$
$$a_{2,0}X(0) + a_{2,1}X(1) + \cdots + a_{2,N-1}X(N-1) = y(2)$$
$$\vdots$$
$$a_{M,0}X(0) + a_{M,1}X(1) + \cdots + a_{M,N-1}X(N-1) = y(M), \tag{5}$$

where $a_{i,k} = \varphi_k(n_i)/N$.

The matrix notation for this system of M linear equations is

$$\mathbf{AX} = \mathbf{y}. \tag{6}$$

The measurement matrix **A**, with elements $a_{i,k}$, is obtained from the inverse DFT matrix $\mathbf{W}^{-1}$, by eliminating the rows corresponding to the unavailable/outlier samples. Notice that the system in (5) or (6) is the general form of the CS setups, for a sparse vector, **X**, related to its measurements, **y**, via the measurement matrix, **A**, which may be random or formed as a partial using any standard linear transform [49]. The method proposed in this paper can be applied to any of them.

The goal of the CS approach is to reconstruct the complete signal $X(k)$, $k = 0, 1, 2, \ldots, N-1$ (or $x(n)$, $n = 0, 1, 2, \ldots, N-1$ if a signal and its linear transform are considered), from the reduced (compressively sensed) subset of measurements (signal samples at the instants n_i, $i = 1, 2, \ldots, M$) with $M < N$. This problem cannot be solved in a direct way, since there are M equations representing M measurements with N unknown transformation domain elements of $X(k)$, such that $M < N$. When the signal sparsity is assumed, the sparsity measure minimization is added to the problem setup. Among an infinite number of solutions for the underdetermined system in (6), $\mathbf{AX} = \mathbf{y}$, we look for the one with the sparsest possible representation in the transformation domain while satisfying the measurement equations. The constrained minimization problem formulation is,

$$\min \|\mathbf{X}\|_0 \text{ subject to } \mathbf{y} = \mathbf{AX}. \tag{7}$$

The solution to this problem exists (if some conditions are met) and it produces the signal transformation elements, $X(k)$, and consequently the signal samples, $x(n)$, at all instants.

Simple counting of the nonzero values of $X(k)$ is achieved using the so-called ℓ_0-norm $\|\mathbf{X}\|_0$. However, the solution based on the ℓ_0-norm is an NP-hard optimization

problem. Its calculation complexity is of order $\binom{N}{K}$. In theory, the NP-hard problems can be solved by an exhaustive search. However, as the problem parameters N and K increase, the computational time increases and the problem becomes unsolvable in a realistic time frame.

Many methods are recently developed for the CS-based reconstruction, by solving the minimization problem (7) or its various equivalent forms (a review of the CS reconstruction methods can be found in [49]). In this paper, we will use a very simple and efficient algorithm that belongs to the class of matching pursuit algorithms. This algorithm will be described in Sect. 3.2.

2.1 RANSAC Review

The random sample consensus (RANSAC) is used for linear regression when the outliers in the data are expected. Outliers are data values that differ significantly from other samples, meaning that they are unusual values in the considered set of samples. A quantitative description of the outliers will be given in the next section.

Consider a set of data $x(n_i)$ sampled at random instants n_i. Assume that the true data values fit a linear model, $x(n) = an + b$. Since some outliers in the dataset can be expected, these data samples will be far from the linear model. In the standard RANSAC approach, we will:

1. Assume a small subset $\mathbb{S}$ with S randomly selected samples $x(n_i)$ at $n_i \in \mathbb{S}$.
2. The samples with indices in $\mathbb{S}$ are used to roughly estimate the linear regression model parameters,

$$\hat{a} \sum_{n_i \in \mathbb{S}} n_i^2 + \hat{b} \sum_{n_i \in \mathbb{S}} n_i = \sum_{n_i \in \mathbb{S}} n_i x(n_i) \quad \text{and} \quad \hat{a} \sum_{n_i \in \mathbb{S}} n_i + \hat{b} N = \sum_{n_i \in \mathbb{S}} x(n_i). \quad (8)$$

3. After the parameters a and b are estimated, the line

$$\hat{x}(n) = \hat{a}n + \hat{b} \quad (9)$$

is defined. The distances d_n of all data points $(n, x(n)), n = 0, 1, \ldots, N - 1$, from this line are calculated, $d_n = |\hat{a}n + \hat{b} - x(n)|/\sqrt{1 + \hat{a}^2}$.
4. If a sufficient number of data points is such that their distance from the model line is lower than an assumed distance threshold d, then all these points are included into a new set of data

$$\mathbb{D} = \{(n_i, x(n_i)) \mid d_{n_i} \leq d\}, \quad (10)$$

and the final parameters a and b (for machine learning or prediction) are calculated with all data from $\mathbb{D}$.
5. If there was no sufficient number of data points within the distance d, a new random small set of data, $\mathbb{S}$, is taken and the procedure is repeated from point 2.
6. The procedure ends when the desired number of data points within $\mathbb{D}$ is achieved or the maximum number of trials is reached.

3 Reconstruction of Sparse Signal with Outliers

Consider a signal $x(n)$, $0 \leq n \leq N - 1$, which is sparse in a transformation domain with a sparsity $K \ll N$. Assume that the signal is noisy with a small noise $\varepsilon(n)$ in all samples. Assume that I samples of the signal $x(n)$, at unknown positions $n \in \mathbb{N}_I$, are corrupted additionally with an impulsive disturbance $\nu(n)$ so that the analyzed signal is $x(n) + \varepsilon(n) + \nu(n)$. The impulsive disturbance $\nu(n)$ can be modeled, for example, as $\nu(n) = 0$ for $n \notin \mathbb{N}_I$ and $\nu(n)$ assumes arbitrary high values for $n \in \mathbb{N}_I$. Signal samples at $n \in \mathbb{N}_I$, with heavy disturbing values, are called outliers. The original signal, $x(n)$, can be recovered if a sufficient number of the inlier samples (with small noise or without noise) exists.

The inliers and outliers are introduced in the previous signal description in an intuitive way. For the quantitative description of these forms of signal disturbances the so-called z-score is used. It is defined as [18]

$$z(n) = \frac{x(n) - \hat{\mu}_x}{\hat{\sigma}_x}, \tag{11}$$

where $\hat{\mu}_x$ is the sample average and $\hat{\sigma}_x$ is the sample standard deviation of the signal $x(n)$, $n = 0, 1, 2, \ldots, N - 1$. In order to declare that a signal value is either inlier or outlier, a threshold T is assumed. The signal samples with the z-score such that $|z(n)| \leq T$ are declared as inliers and the samples with $|z(n)| > T$ as outliers. Since the most common form of small disturbances is the one obeying the Gaussian distribution [18], the threshold value T is assumed between 2 and 3, corresponding to the well-known two-sigma rule and the three-sigma rule. Since the values of the sample average $\hat{\mu}_x$ and the sample standard deviation $\hat{\sigma}_x$ can be significantly compromised with possible impulsive disturbances, it is recommended using the median and the corresponding median absolute deviation (MAD) in the z-score, instead of the sample mean and sample standard deviation. The MAD definition will be provided later.

The sufficient number of inliers for the full signal reconstruction is directly related to the full recovery conditions studied in the CS theory [6,13,26]. A rough estimation of the smallest number of samples that should be used in the reconstruction of K sparse signal can be made based on the statistical results presented in [45]. The exact reconstruction conditions are commonly defined by the restricted isometry property (RIP), using the spark, or the coherence of the measurement matrix [6,13,46,49]. However, these conditions are either computationally unfeasible or too pessimistic. In numerical tests, we followed the set of practical guidelines from [13,46] for situations when one could expect perfect recovery from a partial Fourier matrix using convex optimization. It is suggested that in the case when $K \leq M/5$, the recovery rate is highly reliable. It is worth mentioning that computationally feasible results for the reconstruction uniqueness of signals sparse in the DFT domain are presented in [43], [40].

It is important to emphasize that the use of lower values for M, when some unsuccessful reconstructions are expected to happen, will not be problematic for the RANSAC, since this methodology, by definition, searches for successful reconstruction, as it will be shown in the next section.

3.1 Concentration Measure-Based Denoising

To solve the stated problem, in our previous work [4,5,38,44,45], we exploited the idea of eliminating random subsets of samples and performing the reconstruction using the remaining samples. For each realization, the sparsity measure of the recovered signal is used for the detection of the full recovery event. By using a sparsity measure close to the l_0-norm, all realizations containing disturbed samples will produce a sparsity measure close to the total number of samples N. This is expected, since a disturbance at any signal sample, will affect all coefficients in the sparsity domain [45]. As an illustration, consider a disturbance at n_i, of the form $v(n) = v_0\delta(n - n_i)$, which is added to the signal sample $x(n)$ at n_i. Its DFT, $X_v(k) = v_0 \exp(j2\pi n_i k/N)$, $k = 0, 1, \ldots, N - 1$, is spread over all DFT coefficients of the original signal. In many CS approaches, ℓ_1-norm is used as a measure of signal sparsity [39]. Noise influence on sparsity measures has also been investigated in [20,55].

In the case when only the uncorrupted samples are used in the reconstruction, the sparsity measure is of order K. It is much lower than the total number of samples N. Therefore, by setting a threshold for the sparsity measure between K and N, we can detect a full recovery event.

The main idea behind this approach can be significantly improved, with respect to the detection criterion and the final signal estimation, using an increased number of samples provided by the RANSAC method, which has been extensively applied in machine learning [25,28,56] and signal processing [11].

3.2 RANSAC-Based CS Signal Denoising

In this section, we present the RANSAC-based CS denoising approach. The considered signal model, described at the beginning of this section, is

$$x(n) = s(n) + \varepsilon(n) + v(n),\tag{12}$$

where $s(n)$ is a desired signal sparse in the DFT domain, $\varepsilon(n)$ is a Gaussian noise with variance σ_ε^2, and $v(n)$ is a heavy-tailed impulsive noise with large amplitudes. The Gaussian noise is considered as a small noise and the samples with this kind of noise as inliers. The impulsive noise causes outliers in the signal samples.

For the RANSAC-based denoising, we will use the following algorithm:

1. The considered desired signal $s(n)$ is K-sparse. Randomly select a small subset $\mathbb{S}$ of the time indices, n, with S corresponding samples $x(n)$ at $n \in \mathbb{S}$, such that the reconstruction for a K-sparse signal is theoretically possible with high a probability if the selected samples were noise free, $x(n) = s(n)$, or with small noise only, $x(n) = s(n) + \varepsilon(n)$.

2. The signal samples $x(n)$ with the time indices $n \in \mathbb{S}$ are used to reconstruct the signal, $x_R(n)$, at all instants $n = 0, 1, \ldots, N - 1$. An approach to solve the CS reconstruction problem is a two-step strategy as follows [49]:

   – Step 1: Detect the positions of nonzero elements $X(k)$ in the sparsity domain,

– Step 2: Apply an algorithm for reconstruction with known positions of nonzero elements (use the positions from Step 1).

Next, more details will be provided for this reconstruction approach. The measurements, $x(n)$, are characterized by a linear nature, meaning that they are obtained as linear combinations of the sparsity domain elements, $X(k)$, with the corresponding rows of the measurement matrix, $\mathbf{A}$, acting as weights. As in (4) and (5), we can write

$$y(i) = x(n_i) = \frac{1}{N} \sum_{k=0}^{N-1} a_{i,k} X(k), \quad n_i \in \mathbb{S} \tag{13}$$

or in a matrix form $\mathbf{y} = \mathbf{A}\mathbf{X}$. This implies that a back-projection of the measurements, $\mathbf{y}$, to the measurement matrix, $\mathbf{A}$, defined by

$$\mathbf{X}_0 = \mathbf{A}^H \mathbf{y} = \mathbf{A}^H \mathbf{A}\mathbf{X} \tag{14}$$

can be used to estimate the positions of the nonzero elements in $\mathbf{X}$.

In an ideal case (*one-step reconstruction* algorithm [49]), the matrix $\mathbf{A}^H \mathbf{A}$ should ensure that the initial estimate, $\mathbf{X}_0$, contains exactly K elements at positions $\{k_1, k_2, \ldots, k_K\}$, for which the magnitudes are larger than the largest magnitude at the remaining positions. Under such condition, by taking the positions of these largest magnitude elements in $\mathbf{X}_0$ as the set $\{k_1, k_2, \ldots, k_K\}$, the algorithm for the known nonzero element positions, can be applied to reconstruct the signal using the pseudo-inversion as

$$\mathbf{X}_K = (\mathbf{A}_K^H \mathbf{A}_K)^{-1} \mathbf{A}_K^H \mathbf{y} = \text{pinv}(\mathbf{A}_K)\mathbf{y}, \tag{15}$$

where $\mathbf{A}_K$ is the matrix obtained from the measurement matrix $\mathbf{A}$, by keeping the columns which correspond to the indices $\{k_1, k_2, \ldots, k_K\}$, as elaborated in detail in [49].

The reconstructed signal is

$$x_R(n) = \text{IDFT}\{X_{K0}(k)\} \tag{16}$$

where $X_{K0}(k)$ are zero-valued at all k except $k \in \{k_1, k_2, \ldots, k_K\}$, where $X_{K0}(k_i) = X_K(i)$.

The procedure can be iteratively implemented. In the *iterative procedure*, the largest signal component is detected and estimated first (as it were $K = 1$). The reconstructed component is subtracted from the available measurements, and the modified measurements are used to detect the position of the second largest component. The two largest components are re-estimated together and subtracted from the available measurements. The procedure is continued until the subtraction of the estimated components from the available measurements does not produce sufficiently small (stopping criterion) value or until an assumed sparsity, K, is reached. The iterative implementation is particularly suitable in the case when the nonzero

coefficient values significantly differ. By reconstructing the detected large components, during the iterations, and removing their influence on the previously non-detected components, smaller components will emerge [49].

3. After the signal is reconstructed at all instants, using (16), from a reduced set of samples in (13), the distance d_n of all signal samples $(n, x(n)), n = 0, 1, \ldots, N-1$, from the estimated signal $x_R(n)$ are calculated,

$$d_n = |x_R(n) - x(n)|. \tag{17}$$

4. If there are a sufficient number of signal values with distance from the reconstructed signal (model) being lower than an assumed threshold, for example, for the Gaussian distributed inliers $d = 2.5\sigma_\varepsilon$, then all these points are included in the new set of the signal values

$$\mathbb{D} = \{(n, x(n)) \mid d_n \leq d\}, \tag{18}$$

and the final reconstruction is calculated *with all data from* $\mathbb{D}$. Note that the robust estimation of the standard deviation can be done using the median absolute deviation (MAD), defined by

$$\text{MAD}_x = \underset{m=0,1,\ldots,N-1}{\text{median}}\{|x(m) - \underset{n=0,1,\ldots,N-1}{\text{median}}\{x(n)\}|\}. \tag{19}$$

The MAD value is related to the sample standard deviation, σ_ε, as $MAD_x = 0.6745\sigma_x$ (for the Gaussian random variable). The real and imaginary parts are considered separately for complex-valued signals. In this way we can estimate the standard deviation, σ_ε, needed for the proposed algorithm implementation [21,24].

5. If there was no sufficient number of signal values within the distance d, that is, card$\{\mathbb{D}\} < T = 3N/4$, a new random set of signal sample indices, $\mathbb{S}$, is taken and the procedure is repeated from Step 2. The value T is assumed based on the expected number of outliers. The assumed $T = 3N/4$ means that we do not expect more than $N/4$ outliers.

6. The procedure is stopped when the desired number of data points within $\mathbb{D}$ is achieved, card$\{\mathbb{D}\} \geq T = 3N/4$ or the maximum number of trials N_{max} is reached.

The previously described denoising approach is summarized in Algorithm 1. It exploits a matching pursuit CS reconstruction procedure, CS$_{\text{REC}}$·, summarized in Algorithm 2.

The presented RANSAC-based denoising algorithm will produce the same results if other CS reconstruction methodologies are used, such as, for instance, the Bayesian CS reconstruction or the iterative hard thresholding (IHT). An overview of these procedures, along with their algorithmic presentation, suitable for implementation, can be found in [37,49].

Algorithm 1 RANSAC CS Denoising Algorithm

Input: Noisy signal $\mathbf{x}$, RANSAC set size S, bound for inliers d, threshold for the consensus number of samples T, maximum number of iterations N_{max}, signal sparsity K

1: $D \leftarrow 0$, $N_{it} \leftarrow 0$
2: **while** $D < T$ and $N_{it} \leq N_{max}$ **do**
3:    $N_{it} \leftarrow N_{it} + 1$
4:    $\mathbb{S} \leftarrow \text{randperm}(N, S)$,   ▷ S random numbers from the first N natural numbers
5:    $\mathbf{A} \leftarrow$ rows of the inverse DFT matrix $\mathbf{W}^{-1}$ selected by the set $\mathbb{S}$
6:    $\mathbf{y} \leftarrow$ elements of $\mathbf{x}$ selected by the set $\mathbb{S}$
7:    $\mathbf{X} \leftarrow \text{CS}_{\text{REC}}(\mathbf{y}, \mathbf{A}, K)$
8:    $\mathbf{x}_R = \mathbf{W}^{-1}\mathbf{X}$
9:    $\mathbb{D} = \text{find}(|\mathbf{x} - \mathbf{x}_R| < d)$,
10:   $D = \text{card}(\mathbb{D})$,   ▷ the number of elements in $\mathbb{D}$
11: **end while**

   Perform the CS reconstruction with the consensus set $\mathbb{D}$:

12: $\mathbf{A} \leftarrow$ rows of the inverse DFT matrix $\mathbf{W}^{-1}$ selected by set $\mathbb{D}$
13: $\mathbf{y} \leftarrow$ elements of $\mathbf{x}$ selected by the set $\mathbb{D}$
14: $\mathbf{X} \leftarrow \text{CS}_{\text{REC}}(\mathbf{y}, \mathbf{A}, K)$
15: $\mathbf{x}_R \leftarrow \mathbf{W}^{-1}\mathbf{X}$

Output: Reconstructed denoised signal $\mathbf{x}_R$

Algorithm 2 Matching Pursuit CS Reconstruction

1: **function** CS_{REC}$(\mathbf{y}, \mathbf{A}, K)$
2:    $\mathbb{K} \leftarrow \emptyset$, $\mathbf{e} \leftarrow \mathbf{y}$,
3:    **for** $i = 1$ to K **do**
4:       $k \leftarrow$ position of the largest value in $|\mathbf{A}^H\mathbf{e}|$
5:       $\mathbb{K} \leftarrow \mathbb{K} \cup k$
6:       $\mathbf{A}_K \leftarrow$ columns of the measurement matrix $\mathbf{A}$ selected by the set $\mathbb{K}$
7:       $\mathbf{X}_K \leftarrow \text{pinv}(\mathbf{A}_K)\mathbf{y}$
8:       $\mathbf{y}_K \leftarrow \mathbf{A}_K\mathbf{X}_K$
9:       $\mathbf{e} \leftarrow \mathbf{y} - \mathbf{y}_K$
10:   **end for**
11:   $\mathbf{X} \leftarrow 0$, $\mathbf{X} \leftarrow \mathbf{X}_K$ for $k \in \mathbb{K}$
12:   **return** $\mathbf{X}$
13: **end function**

3.3 Calculation Complexity

The main difference between RANSAC and the standard CS methods is in the iterative procedure with random subsets of samples. Since this is the main factor in the computational complexity of this method, we will find the probability that within S randomly selected observation samples, there are no outliers.

The probability that the first randomly chosen sample is not affected by an outlier is $(N - I)/N$ since there are N samples in total and $N - I$ of them are inliers. We continue the process of random sample selection, and the probability that both the first and the second chosen samples are not outliers is $\frac{N-I}{N}\frac{N-I-1}{N-1}$. In this way, we can calculate the probability that all of S randomly chosen samples $x(n)$ at the positions

$n \in \mathbb{S}$ are not outliers. This probability is

$$P(S, N, I) = \prod_{i=0}^{S-1} \frac{N - I - i}{N - i}.$$

(20)

Since $\frac{N-I-i}{N-i} < 1$, we can see that the probability $P(S, N, I)$ decreases as the number of terms in the product increases. Thus, in this kind of reconstruction it is important to keep the number of samples S in the observation set as low as possible, while satisfying the CS reconstruction conditions.

In general, for an expected number of pulses I, the expected number of random realizations to achieve at least one outlier-free reconstruction using a subset of S samples is

$$N_{it} = \frac{1}{P(S, N, I)}.$$

(21)

In classic literature dealing with the RANSAC, it is common to use the following calculation for the expected number of the iterations to get an outlier-free realization. The probability that one randomly selected sample is inlier is $(N - I)/N$. It is then assumed that this probability can be used for S samples. The probability that there is at least one outlier in S samples is $[1 - ((N - I)/N))^S]$. Finally, the probability of an outlier-free realization in N_{it} such trials is

$$P = 1 - [1 - ((N - I)/N)^S]^{N_{it}}$$

(22)

where

$$N_{it} = \frac{\ln(1 - P)}{\ln(1 - ((N - I)/N)^S)},$$

(23)

with the given probability P. This calculation is correct if the approximation

$$\frac{N - I - S}{N - S} \approx \frac{N - I}{N},$$

(24)

holds; otherwise, instead of $((N - I)/N)^S$ we should use $P(S, N, I) = \prod_{i=0}^{S-1} (N - I - i)/(N - i)$ to get the correct result.

3.4 Expected Signal-to-Noise Ratio

Assume that the RANSAC has produced the correct result, that is, the reconstruction which is not influenced by the outliers. This means that the final reconstruction is done using all consensus samples in the set $\mathbb{D}$. This set of samples contains only inliers (with the Gaussian noise). Then, we can use a simple formula for the output SNR in the K-sparse signal, reconstructed from D samples, SNR_{out}, derived in [44,47,49]

$$SNR_{out} = SNR_{in0} + 10\log\left(\frac{D}{K}\right). \tag{25}$$

Since the outliers are eliminated before the reconstruction, the input SNR is denoted by SNR_{in0} and it includes the noise in inliers only. For reference, we will provide the total input SNR in notation SNR_{in}, which includes outliers as well. We will also provide the value of the SNR in the mid-result, when the sample consensus is reached in a small subset $\mathbb{S}$ with S samples. This SNR is denoted by SNR_{out0} and its relation to the input SNR is

$$SNR_{out0} = SNR_{in0} + 10\log\left(\frac{S}{K}\right). \tag{26}$$

The improvement achieved by the RANSAC-based approach with respect to the random selection of the subsets and the concentration measure-based selection of the reconstruction set, is equal to

$$SNR_{out} - SNR_{out0} = 10\log\left(\frac{D}{K}\right) - 10\log\left(\frac{S}{K}\right) = 10\log\left(\frac{D}{S}\right). \tag{27}$$

This improvement can be significant, having in mind that we have to keep S as small as possible, in order to reduce the expected number of iterations N_{it}, which is crucial for the calculation complexity, for both the measure-based denoising and the RANSAC-based denoising. The number of consensus samples, D, can be as high as the number of inliers, meaning that the ratio D/S could be very large.

4 Numerical and Statistical Examples

The results from the last two sections will now be illustrated on numerical and statistical examples with sparse noisy signals, containing inliers and outliers, reconstructed using the CS version of the RANSAC.

Example 1 A general form of a noisy signal, sparse in the DFT domain, is considered as

$$x(n) = s(n) + \varepsilon(n) + v(n), \tag{28}$$

where

$$s(n) = \sum_{i=1}^{K} A_k e^{j(2\pi nk_i/N + \phi_k)} \tag{29}$$

is a signal sparse in the DFT domain with K nonzero amplitudes randomly positioned at $\{k_1, k_2, \ldots, k_K\}$. The amplitude values are equal to one, $A_k = 1$, since the same amplitudes are the worst case in the CS reconstruction condition [46,49]. The phases,
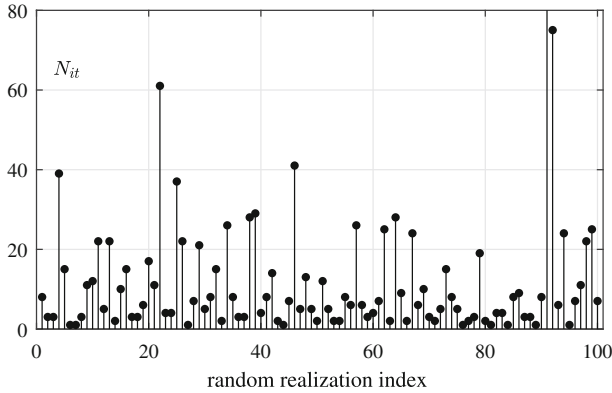
Fig. 1 The number of iterations N_{it} in the reconstruction of a signal using the RANSAC, with $I = 16$ out of $N = 128$ samples being affected by an impulsive Cauchy disturbance. The average value is 11.99
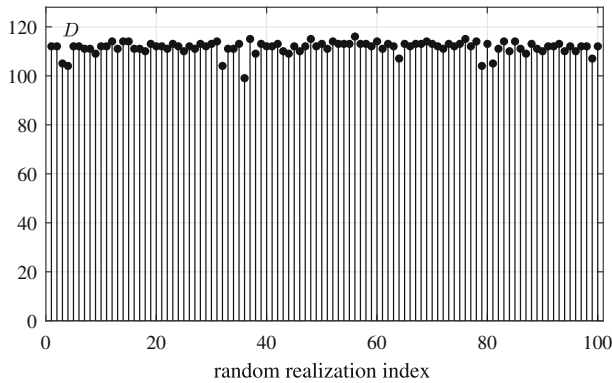

Fig. 2 The number of inliers in the solution in the reconstruction of a signal using the RANSAC, with $I = 16$ out of $N = 128$ samples being affected by an impulsive Cauchy disturbance. The average value is 111.33

ϕ_k, are random and uniformly distributed, $0 \leq \phi_k < 2\pi$, for each component and realization. The Gaussian complex-valued noise $\varepsilon(n)$ is with the standard deviation $\sigma_\varepsilon = 0.5$. The impulsive Cauchy noise $\nu(n)$ is formed as $\nu(n) = 3\varepsilon_1(n)/\varepsilon_2(n) + j3\varepsilon_3(n)/\varepsilon_4(n)$, where $\varepsilon_i(n)$, $i = 1, 2, 3, 4$ are unit variance, zero-mean, Gaussian noises. The impulsive noise is added in I signal samples. In the denoising of this signal, the CS form of the RANSAC is applied with random subsets of S samples, where S is small enough to keep the lowest possible calculation complexity, but sufficient to provide the correct reconstruction of a K sparse signal with acceptable probability.

Several cases, for specific values of the total number of samples, N, sparsity, K, number of outliers, I, and the size of the RANSAC subset, S, are considered.

The case for $N = 128$, $K = 5$, $I = 16$, and $S = 32$ is presented in detail with illustrations in Figs. 1, 2, 3, and 4. This experiment is performed 100 times with different random realizations of signals, $x(n)$, and noises, $\varepsilon(n)$ and $\nu(n)$. The values of the number of iterations, N_{it}, in every realization are calculated and shown in
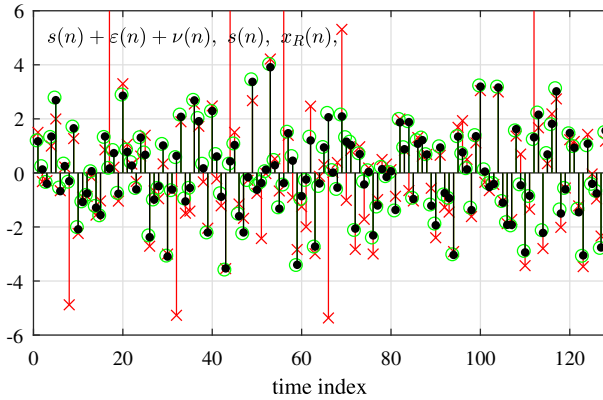
Fig. 3 Reconstruction of a signal with $I = 16$ out of $N = 128$ samples using the RANSAC, being affected by an impulsive Cauchy disturbance. One random realization is shown for the illustration. The noisy signal is marked by the red crosses, and the reconstructed signals are denoted by the green circles, while the original signal is shown with the black dots (Colour figure online)
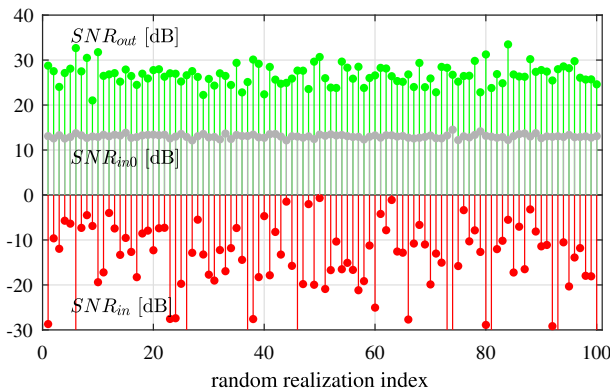

Fig. 4 The signal-to-noise ratio values in the reconstruction of a sparse signal using the RANSAC with $I = 16$ samples (out of $N = 128$) being affected by an impulsive Cauchy disturbance. The average values are $SNR_{in} = -16.73$ dB for the input signal to noise, $SNR_{in0} = 13.00$ dB for the input signal to Gaussian noise (when the impulsive noise is not counted), and $SNR_{out} = 26.46$ dB for the RANSAC reconstructed (output) signal

Fig. 1. The final number of signal samples in the sample consensus, D, which is used in the final signal reconstruction is given in Fig. 2. One of the realizations of the noisy signal, original signal, and the reconstructed signal is shown in Fig. 3. The noisy signal is marked by the red crosses, the reconstructed signal is denoted by the green circles, while the original signal is shown with the black dots. The SNR for the input signal $s(n) + \varepsilon(n) + \nu(n)$, SNR_{in}, for the input signal without impulsive noise $s(n) + \varepsilon(n)$, SNR_{in0}, and for the reconstructed signal $x_R(n)$, SNR_{out}, for every realization, is given in Fig. 4.

The statistical results averaged over all considered realizations are given in Table 1.

Table 1 Results for the case with $N = 128$, $S = 32$, $K = 5$

	N_{it}	SNR_{in}	SNR_{in0}	SNR_{out0}	SNR_{out}	D	Time
$I = 8$	2.94	−8.81	13.01	16.23	27.07	119.46	0.010
$I = 16$	11.99	−16.73	13.00	14.39	26.46	111.33	0.038
$I = 24$	57.66	−17.53	13.01	13.29	25.91	103.56	0.201

The SNR values are given in [dB], while the average time for the algorithm execution (with MATLAB 2016b on MacBook Pro with 2.3 GHz Dual-Core Intel Core i5) is in seconds

The theoretically expected improvement (Sect. 3.4) in the SNR (omitting the impulsive noise in the input signal) for the case $I = 8$, in Table 1, is

$$SNR_{out} - SNR_{in0} = 10 \log \left(\frac{D}{K} \right) = 10 \log \left(\frac{119.46}{5} \right) = 13.77 dB \qquad (30)$$

For other two cases, $I = 16$ and $I = 24$, we get

$$SNR_{out} - SNR_{in0} = 13.46 dB \qquad (31)$$

and $SNR_{out} - SNR_{in0} = 13.14$ dB, respectively. This is in high agreement with the statistical data in Table 1.

The average processing time for the algorithm is shown in Table 1 (the last column) for the considered cases, along with the specification of the computer and MATLAB. As expected, the main computation burden is in the combinatorial search for a reduced set of signal samples without outliers (which includes the CS reconstruction in each iteration step), meaning that the processing time can roughly be approximated based on the required number of iterations, shown in the first column of the results.

Example 2 Since the impulsive Cauchy noise may take some small values as well (some of the assumed I outliers may happen to be inliers, in reality), the expected number of iterations is smaller than the theoretically obtained result given by (20). In order to check the expected number of iterations, N_{it}, against its theoretical value, avoiding the ambiguity of possible Cauchy noise inliers, we will provide that all I signal samples are certainly outliers. The impulsive noise is modified as $v(n) \rightarrow v(n) + 100$, to be sure that all of these samples are the outliers. Then, we have repeated the same experiment with 100 realizations and obtained $N_{it} = 10.74$, while the theory in (20) predicts $P = 0.0927$ with $N_{it} = 1/P = 10.78$, for $I = 8$. The same numerical experiment as in Example 1 is performed for $I = 16$, and we get $P = 0.0071$ with $N_{it} = 1/P = 140.95$, while the statistics for this case produced $N_{it} = 139.78$. The same holds for $I = 24$. The complete results of the experiment, with the modified impulsive noise, are given in Table 2.

In this case (of the modified impulsive noise), we can also check the result for the SNR in the final RANSAC mid-result, when the consensus is detected on a small subset with S samples. Then,

Table 2 Results for the case with $N = 128$, $S = 32$, $K = 5$, with highly impulsive noise so that all its values are outliers

	N_{it}	SNR_{in}	SNR_{in0}	SNR_{out0}	SNR_{out}	D
$I = 8$	10.74	-22.45	13.01	21.02	27.20	119.96
$I = 16$	139.78	-26.75	13.00	21.06	27.05	111.94
$I = 24$	2335.67	-27.21	13.01	20.71	26.31	103.56

Table 3 Results for the case with $N = 128$, $S = 64$, $K = 12$

	N_{it}	SNR_{in}	SNR_{in0}	SNR_{out0}	SNR_{out}	D
$I = 8$	5.40	-5.24	16.79	14.90	26.30	107.52
$I = 12$	15.06	-10.13	16.76	13.33	25.79	104.85
$I = 16$	99.47	-11.42	16.80	13.10	25.41	101.41

Table 4 Results for the case with $N = 256$, $S = 64$, $K = 12$

	N_{it}	SNR_{in}	SNR_{in0}	SNR_{out0}	SNR_{out}	D
$I = 16$	5.36	-8.63	16.83	15.79	29.14	231.65
$I = 32$	61.84	-14.55	16.84	14.15	28.30	214.07
$I = 40$	261.30	-16.90	16.81	14.42	28.25	208.48

$$SNR_{out0} - SNR_{in0} = 10\log\left(\frac{S}{K}\right) = 10\log\left(\frac{32}{5}\right) = 8.06 \text{ dB} \qquad (32)$$

for all three considered cases, $I = 8$, $I = 16$, and $I = 24$. This result is in complete agreement with the statistical results for these SNR values in Table 2.

Example 3 The experiment form Example 1 is repeated with some other numbers of the available samples, N, sparsites, K, the number of impulsive disturbances, I, and the samples used in the RANSAC-based CS reconstruction. The results are given in Tables 3 and 4 and further prove the efficiency of the proposed method and accuracy of the proposed SNR descriptors.

Example 4 The experiment from Example 1 is repeated with the impulsive noise only, that is, when $x(n) = s(n) + v(n)$. As expected, for all considered numbers of outliers, the obtained results are within the computer precision accuracy. They are given in Table 5. In this case, the value of d should be very small. We used $d = 10^{-6}$ for this experiment.

Example 5 In this example, the presented RANSAC-based methodology is compared with an advanced method developed for the removal of "clicks and pops" from audio signals, proved as superior in comparison with other state-of-art techniques [8,27].

Birkhäuser

Table 5 Results for the case with $N = 128$, $S = 32$, $K = 5$, with highly impulsive noise in outliers and without noise in inliers

	N_{it}	SNR_{in}	SNR_{in0}	SNR_{out0}	SNR_{out}	D
$I = 8$	10.68	-22.44	316.64	276.25	282.12	120
$I = 16$	138.21	-26.75	316.67	271.86	277.52	112
$I = 24$	2402.23	-27.47	316.67	270.51	275.40	104

In our example, a recorded signal containing spoken word 'Hallelujah' is considered. Signal is recorded on a MacBook computer using MATLAB with sampling frequency 11025Hz. The recorded signal is corrupted with additive impulsive noise of the form $\sigma \epsilon_1(n)/\epsilon_2(n)$, with $\epsilon_1(n)$ and $\epsilon_2(n)$ being white, Gaussian noises with mean values equal zero and unit variances. Two cases are considered: (i) A small percent of $p = 1\%$ samples is corrupted, with $\sigma = 0.008$ and (ii) a higher percent of $p = 8\%$ samples is corrupted, with $\sigma = 0.0035$.

We compare the RANSAC-based recovery with the recent method for impulsive noise (clicks) detection and removal (AR-based reconstruction), presented in [8,27]. The detection and the AR model-based reconstruction are done using authors' algorithms, codes and parameters (semi-causal with decision-feedback scheme) [8]. The bidirectional signal processing (BDSP), originally introduced in [27] is considered as a representative methodology. This algorithm is highly adapted for the removal of this kind of impulsive disturbances in audio signals.

The results are presented in Figs. 5 and 6. In the first case with 1% corrupted samples, the BDSP produced MSE of -48.21dB, while RANSAC-based reconstruction MSE is slightly improved to -51.17, where $d = 0.02$ and assumed sparsity $K = 35$ is used. In this analysis the DCT was used as the sparsity domain. The initial MSE in the signal was -33.72dB Reconstruction times are 18.04s and 37.27s, meaning that the BDSP is computationally more efficient in this case. Algorithms were executed on a notebook computer with Intel i7-6700HQ CPU @ 2.6GHz and 8GB RAM, with MATLAB R2016b.

In the second considered case, as it can be seen from Fig. 6, the proposed RANSAC-based approach produced significantly better results. This can be explained by the fact that BDSP is adapted for specific impulsive disturbances in audio signals of the form of 'clicks', which appear in a very small percent of samples. In the second case, the initial MSE was $-25.16dB$. BDSP produced false detection/increase of the disturbance at certain positions, producing MSE increase to -17.43dB, while RANSAC-based denoising produced significantly better results: MSE is now decreased to -47.90dB close to the first case with a smaller percent of impulsive disturbances. Execution times were 34.30s for RANSAC-based approach, and 19.11s for the BDSP, meaning that the computational ratio is the same as in the first case. The RANSAC-based approach can produce high quality output even if the percent of impulsive disturbances is further increased.

We have compared RANSAC-based approach with our earlier algorithm, from [7]. RANSAC introduced mild improvement in the MSE, but there is a significant
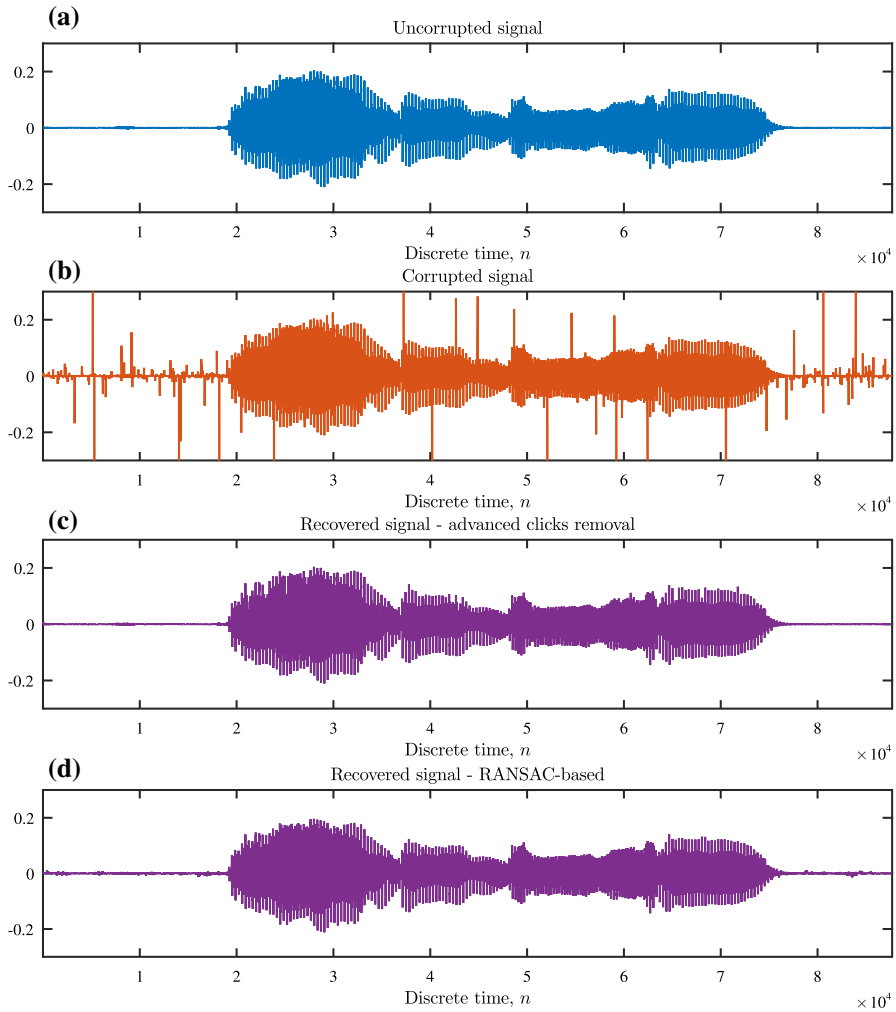
Fig. 5 Removal of impulsive noise from recorded audio signal with 1% of corrupted samples. **a** Original (non-corrupted) audio signal. **b** Signal with 1% samples corrupted by an impulsive disturbance. **c** Signal recovered using advanced bidirectional signal processing technique for the removal of clicks. **d** Signal recovered using the presented RANSAC-based methodology

difference in the computational complexity: RANSAC executes tens of times faster than our earlier approach.

5 Conclusion

Inspired by recent advances in compressive sensing and sparse signal processing, we have developed a RANSAC-based methodology for the detection of disturbances. Upon detecting disturbance-free samples, a compressive sensing algorithm is used
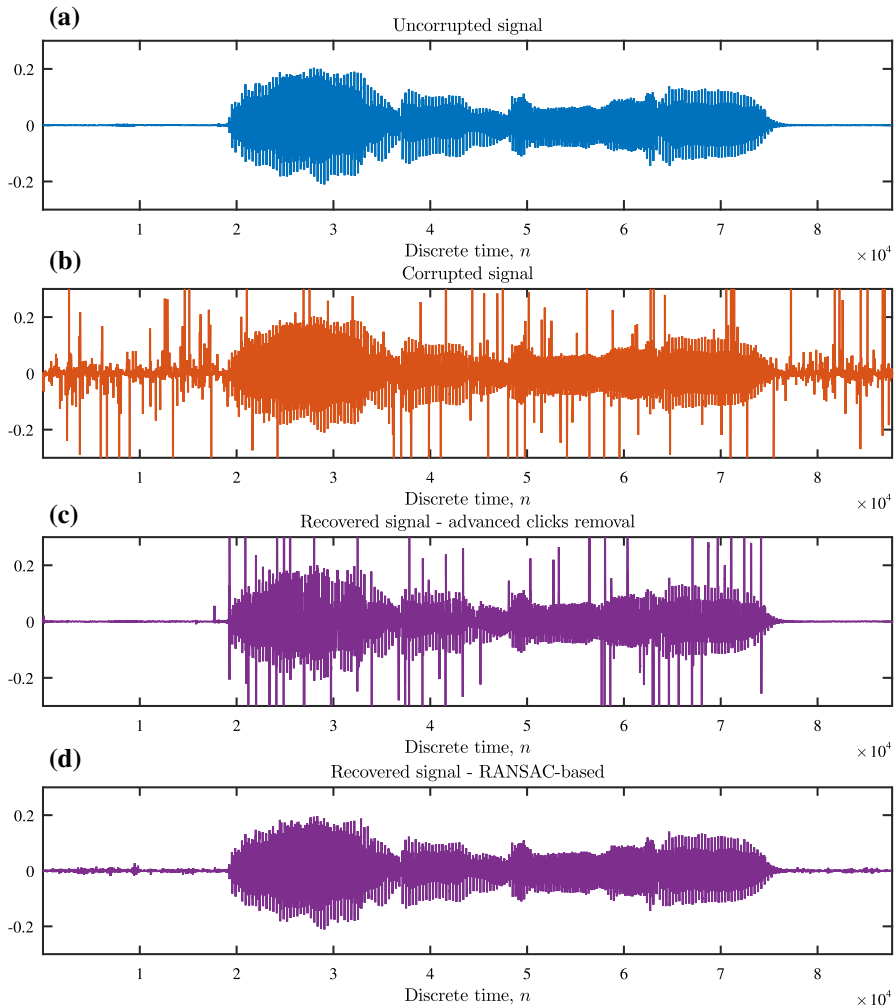
(a)

Fig. 6 Removal of impulsive noise from recorded audio signal with 8% of corrupted samples. **a** Original (non-corrupted) audio signal. **b** Signal with 8% samples corrupted by an impulsive disturbance. **c** Signal recovered using advanced bidirectional signal processing technique for the removal of clicks. **d** Signal recovered using the presented RANSAC-based methodology

for the recovery of the disturbed samples, which are considered as unavailable. The presented methodology is general—no specific assumptions have been made regarding the range of values or statistical behavior of the disturbance. The presented approach exploits the fact that disturbances degrade signal sparsity. It has been only assumed that the signals of interest exhibit sparsity in a known transformation domain. The theory has been verified on numerical examples.

Birkhäuser

Data Availability Data will be made available on reasonable request.

References

1. M.S. Ahmad, O. Kukrer, A. Hocanin, Robust recursive inverse adaptive algorithm in impulsive noise. Circuits Syst. Signal Process. **31**(2), 703–710 (2012)
2. F.R. Avila, L.W.P. Biscainho, Bayesian restoration of audio signals degraded by impulsive noise modeled as individual pulses. IEEE Trans. Audio Speech Lang. Process. **20**(9), 2470–2481 (2012). https://doi.org/10.1109/TASL.2012.2203811
3. T. Blumensath, Sampling and reconstructing signals from a union of linear subspaces. IEEE Trans. Inf. Theory **57**(7), 4660–4671 (2011)
4. M. Brajovic, S. Stankovic, I. Orovic, M. Dakovic, L. Stankovic, Sparsity-Driven Impulsive Noise Removal: A Discrete Hermite Transform Case Study *27th Telecommunications Forum (TELFOR 2019)* (Belgrade, Serbia, 2019)
5. M. Brajovic, I. Stankovic, M. Dakovic, L. Stankovic, The DCT domain sparsity-assisted detection and recovery of impulsively disturbed samples. Multimedia Tools Appl. (2020). https://doi.org/10.1007/s11042-020-09998-w
6. E.J. Candès, J. Romberg, T. Tao, Robust uncertainty principles: exact signal reconstruction from highly incomplete frequency information. IEEE Trans. Inf. Theory **52**(2), 489–509 (2006)
7. R.E. Carrillo, K.E. Barner, T.C. Aysal, Robust sampling and reconstruction methods for sparse signals in the presence of impulsive noise. IEEE J. Select. Top. Signal Process. **4**(2), 392–408 (2010)
8. M. Ciołek , M. Niedźwiecki, Detection of impulsive disturbances in archive audio signals. *2017 IEEE International Conference on Acoustics, Speech and Signal Processing (ICASSP)*, New Orleans, LA (2017), pp. 671–675. https://doi.org/10.1109/ICASSP.2017.7952240
9. F. Dadouchi, C. Gervaise, C. Ioana, J. Huillery, J.I. Mars, Automated segmentation of linear time-frequency representations of marine-mammal sounds. J. Acoust. Soc. Am. **134**(3), 2546–2555 (2013)
10. G. Davis, S. Mallat, M. Avellaneda, Adaptive greedy approximations. Constr. Approx. **13**(1), 57–98 (1997)
11. I. Djurovic, A WD-RANSAC instantaneous frequency estimator. IEEE Signal Process. Lett. **23**(5), 757–761 (2016)
12. I. Djurovic, V.V. Lukin, M. Simeunovic, B. Barkat, Quasi maximum likelihood estimator of polynomial phase signals for compressed sensed data. AEU-Int. J. Electron. Commun. **68**(7), 631–636 (2014)
13. D.L. Donoho, Compressed sensing. IEEE Trans. Inf. Theory **52**(4), 1289–1306 (2006)
14. K. Egiazarian, A. Foi , V. Katkovnik, Compressed sensing image reconstruction via recursive spatially adaptive filtering, in *2007 IEEE International Conference on Image Processing*, San Antonio, TX, pp. 549–552 (2007), https://doi.org/10.1109/ICIP.2007.4379013
15. M.J. Fadili, J.L. Starck, F. Murtagh, Inpainting and zooming using sparse representations. Comput. J. **52**(1), 64–79 (2009)
16. R. Feng, Q. Du, X. Li, H. Shen, Robust registration for remote sensing images by combining and localizing feature- and area-based methods. ISPRS J. Photogramm. Remote Sens. **151**, 15–26 (2019)
17. P. Flandrin, P. Borgnat, Time-frequency energy distributions meet compressed sensing. IEEE Trans. Signal Process. **58**(6), 2974–2982 (2010)
18. F.E. Grubbs, Procedures for detecting outlying observations in samples. Technometrics **11**(1), 1–21 (1969)
19. R. Hu, Y. Fu, Z. Chen, Y. Xiang, J. Tang, A Lorentzian IHT for complex-valued sparse signal recovery. Circuits Syst. Signal Process. **37**(2), 862–872 (2018)
20. B. Jokanovic, M.G. Amin, Y.D. Zhang, Reducing noise in the time-frequency representation using sparsity promoting kernel design, in *Proceedings of SPIE 9109, Compressive Sensing III (91090B)* (2014), https://doi.org/10.1117/12.2050894
21. V. Katkovnik, L. Stankovic, Instantaneous frequency estimation using the Wigner distribution with varying and data driven window length. IEEE Trans. Signal Process. **46**(9), 2315–2325 (1998)
22. N.A. Khan, M. Mohammadi, Reconstruction of non-stationary signals with missing samples using time-frequency filtering. Circuits Syst. Signal Process. **37**(8), 3175–3190 (2018)
23. T. Kim, Y.J. Im, Automatic satellite image registration by combination of matching and random sample consensus. IEEE Trans. Geosci. Remote Sens. **41**(5), 1111–1117 (2003). https://doi.org/10.1109/TGRS.2003.811994

24. C. Leys, C. Ley, O. Klein, P. Bernard, L. Licata, Detecting outliers: do not use standard deviation around the mean, use absolute deviation around the median. J. Exp. Soc. Psychol. **49**(4), 764–766 (2013)
25. J. Matas, O. Chum, Randomized RANSAC with T(d,d) test, in ed. D. Marshall, P. L. Rosin, *Proceedings of the British Machine Conference*, 43.1–43.10, (BMVA Press 2002), https://doi.org/10.5244/C.16.43.
26. D. Needell, J.A. Tropp, CoSaMP: Iterative signal recovery from incomplete and inaccurate samples. Appl. Comput. Harmon. Anal. **26**(3), 301–321 (2009)
27. M. Niedźwiecki, M. Ciołek, Elimination of Impulsive Disturbances From Archive Audio Signals Using Bidirectional Processing. IEEE Trans. Audio Speech Lang. Process. **21**(5), 1046–1059 (2013). https://doi.org/10.1109/TASL.2013.2244090
28. D. Nister, Preemptive RANSAC for live structure and motion estimation, in *Proceedings Ninth IEEE International Conference on Computer Vision Nice*, France (2003), pp. 199–206, https://doi.org/10.1109/ICCV.2003.1238341
29. I. Orovic, V. Papic, C. Ioana, X. Li, S. Stankovic, Compressive sensing in signal processing: algorithms and transform domain formulations. Math. Probl. Eng. (2016)
30. Z.M. Ramadan, Efficient restoration method for images corrupted with impulse noise. Circuits Syst. Signal Process. **31**(4), 1397–1406 (2012)
31. A.A. Roenko, V.V. Lukin, I. Djurovic, Two approaches to adaptation of sample myriad to characteristics of SαS distribution data. Sig. Process. **90**(7), 2113–2123 (2010)
32. M. Ruhland, J. Bitzer, M. Brandt, S. Goetze, Reduction of gaussian, supergaussian, and impulsive noise by interpolation of the binary mask residual. IEEE/ACM Trans. Audio Speech Lang. Process. **23**(10), 1680–1691 (2015)
33. E. Sejdic, A. Cam, L. Chaparro, C. Steele, T. Chau, Compressive sampling of swallowing accelerometry signals using time-frequency dictionaries based on modulated discrete prolate spheroidal sequences. EURASIP J. Adv. Signal Process. **101**, 1–14 (2012)
34. H. Shen, X. Li, L. Zhang, D. Tao, C. Zeng, Compressed sensing-based inpainting of aqua moderate resolution imaging spectroradiometer band 6 using adaptive spectrum-weighted sparse Bayesian dictionary learning. IEEE Trans. Geosci. Remote Sens. **52**(2), 894–906 (2014). https://doi.org/10.1109/TGRS.2013.2245509
35. M. Siu, A. Chan, A Robust Viterbi algorithm against impulsive noise with application to speech recognition. IEEE Trans. Audio Speech Lang. Process. **14**(6), 2122–2133 (2006). https://doi.org/10.1109/TASL.2006.872592
36. I. Stankovic, Recovery of images with missing pixels using a gradient compressive sensing algorithm. arXiv preprint arXiv:1407.3695 (2014)
37. I. Stankovic, M. Brajovic, M. Dakovic, C. Ioana, L. Stankovic, Quantization in compressive sensing: a signal processing approach. IEEE Access **8**, 50611–50625 (2020). https://doi.org/10.1109/ACCESS.2020.2979935
38. I. Stankovic, I. Orovic, M. Dakovic, S. Stankovic, Denoising of sparse images in impulsive disturbance environment. Multimed. Tools Appl. **77**(5), 5885–5905 (2018)
39. L. Stankovic, A measure of some time-frequency distributions concentration. Sig. Process. **81**(3), 621–631 (2001)
40. L. Stankovic, *Digital Signal Processing with Selected Topics* (CreateSpace Independent Publishing Platform, An Amazon. Com Company, 2015)
41. L. Stankovic, M. Brajovic, Analysis of the reconstruction of sparse signals in the DCT domain applied to audio signals. IEEE/ACM Trans. Audio Speech Lang. Process. **26**(7), 1216–1231 (2018)
42. L. Stankovic, M. Brajovic, I. Stankovic, C. Ioana, M. Dakovic, Reconstruction error in nonuniformly sampled approximately sparse signals. IEEE Geosci. Remote Sens. Lett. (2020). https://doi.org/10.1109/LGRS.2020.2968137
43. L. Stankovic, M. Dakovic, On the uniqueness of the spa rse signals reconstruction based on the missing samples variation analysis. Math. Probl. Eng. Article ID 629759 (2015). https://doi.org/10.1155/2015/629759
44. L. Stankovic, M. Dakovic, I. Stankovic, S. Vujovic, On the errors in randomly sampled nonsparse signals reconstructed with a sparsity assumption. IEEE Geosci. Remote Sens. Lett. **14**(12), 2453–2456 (2017)
45. L. Stankovic, M. Dakovic, S. Vujovic, Reconstruction of Sparse signals in impulsive disturbance environments. Circuits Syst. Signal Process. **36**, 767–794 (2016). https://doi.org/10.1007/s00034-016-0334-3

46. L. Stankovic, D.P. Mandic, M. Dakovic, I. Kisil, Demystifying the Coherence Index in Compressive Sensing. IEEE Signal Process. Mag. **37**(1), 152–162 (2020)
47. S. Stankovic, I. Orovic, L. Stankovic, An automated signal reconstruction method based on analysis of compressive sensed signals in noisy environment. Sig. Process. **104**, 43–50 (2014)
48. L. Stankovic, I. Orovic, S. Stankovic, M.G. Amin, Compressive sensing based separation of non-stationary and stationary signals overlapping in time-frequency. IEEE Trans. Signal Process. **61**(18), 4562–4572 (2013). https://doi.org/10.1109/TSP.2013.2271752
49. L. Stankovic, E. Sejdic, S. Stankovic, M. Dakovic, I. Orovic, A Tutorial on Sparse Signal Reconstruction and Its Applications in Signal Processing. Circuits Syst. Signal Process. **38**, 1206–1263 (2019). https://doi.org/10.1007/s00034-018-0909-2
50. L. Stankovic, S. Stankovic, M.G. Amin, Missing samples analysis in signals for applications to L-estimation and compressive sensing. Sig. Process. **94**, 401–408 (2014)
51. L. Stankovic, S. Stankovic, I. Orovic, M.G. Amin, Robust time-frequency analysis based on the L-estimation and compressive sensing. IEEE Signal Process. Lett. **20**(5), 499–502 (2013)
52. C. Studer, P. Kuppinger, G. Pope, H. Bolcskei, Recovery of sparsely corrupted signals. IEEE Trans. Inf. Theory **58**(5), 3115–3130 (2012)
53. A. Torokhti, P. Howlett, H. Laga, Estimation of stochastic signals under partially missing information. Sig. Process. **111**, 199–209 (2015)
54. S.V. Vaseghi, *Advanced Digital Signal Processing and Noise Reduction* (Wiley, Hoboken, 2008)
55. I. Volaric, V. Sucic, On the noise impact in the L1 based reconstruction of the sparse time-frequency distributions, in *2016 International Conference on Broadband Communications for Next Generation Networks and Multimedia Applications (CoBCom), Gratz*, pp. 1–6 (2016)
56. H. Wang, D. Suter, Robust adaptive-scale parametric model estimation for computer vision. IEEE Trans. Pattern Anal. Mach. Intell. **26**(11), 1459–1474 (2004). https://doi.org/10.1109/TPAMI.2004.109
57. G.H. You, T.S. Qiu, A.M. Song, Novel direction findings for cyclostationary signals in impulsive noise environments. Circuits Syst. Signal Process. **32**(6), 2939–2956 (2013)
58. L. Zhao, Y. Hu, Y. Liu, Stochastic gradient matching pursuit algorithm based on sparse estimation. Electronics **8**(2), 165 (2019)

Publisher's Note Springer Nature remains neutral with regard to jurisdictional claims in published maps and institutional affiliations.

Affiliations

Ljubiša Stanković[1] · **Miloš Brajović[1]** · **Isidora Stanković[1]** · **Jonatan Lerga[2]** · **Miloš Daković[1]**

✉ Ljubiša Stanković
ljubisa@ucg.ac.me

Miloš Brajović
milosb@ucg.ac.me

Isidora Stanković
isidoras@ucg.ac.me

Jonatan Lerga
jlerga@riteh.hr

Miloš Daković
milos@ucg.ac.me

[1] University of Montenegro, Podgorica, Montenegro

[2] Faculty of Engineering and Center for Artificial Intelligence and Cybersecurity, University of Rijeka, Rijeka, Croatia